

ENERGY MANAGEMENT STRATEGIES FOR FUEL CELL-HYBRID VEHICLES

Diego Feroldi^{}, Enric Roig, Maria Serra, Jordi Riera*

Institut de Robòtica i Informàtica Industrial (IRI)

Consell Superior d'Investigacions Científiques (CSIC)-Universitat Politècnica de

Catalunya (UPC)

Llorens i Artigas, 4-6, Planta 2, 08028, Barcelona

{dferoldi, eroig, maserra, riera}@iri.upc.edu

Abstract: This paper presents an analysis and a comparative study between three new proposed Energy Management Strategies oriented to Fuel Cell-Hybrid Vehicles (FCHVs). The vehicle in study is powered by a fuel cell and a supercapacitor bank that can be charged both from the fuel cell and from the load through regenerative braking. The proposed strategies were tested using a FCHV model elaborated employing ADVISOR toolbox in Matlab. A comparative of the hydrogen consumptions is performed with respect to the optimal case, which is estimated assuming that the entire future driving load demand is known. The results indicate that it is possible to achieve a performance close to the optimal case without knowing the driving cycle a priori. In addition to the hydrogen economy improvement, the strategies allow reducing the fuel cell stack dimension with the consequent reduction in the production costs.

Keywords: Fuel Cell, PEMFC, Energy Management Strategy, Hybrid Vehicle

^{*} Corresponding author: Tel.: +34 93 4015754; fax: +34 93 4015750.
E-mail address: dferoldi@iri.upc.edu (D. Feroldi).

1. INTRODUCTION

Given the present environmental problems and the anticipated fuel shortage for the next decades it is important to find more efficient forms of using the energy resources affecting minimally the environment. According to different studies, such as [1], global oil reserves are only sufficient for around 40 years with the current level of oil production and consumption. Thus, it is important to promote the development of new energy technologies. In this context, hydrogen-based fuel cell technology is a promising alternative because of its high efficiency and environmental benefits.

The main aims of the energy management in fuel cell-based systems are to reduce the hydrogen consumption and to improve the dynamic behaviour. Effectively, the fuel cell efficiency is dependent on the power load, being strongly degraded at low powers. Besides, the transient response of the fuel cell generated power is limited by the fuel cell manifold filling dynamics and the compressor inertia dynamics. In automotive and stand-alone residential applications the load changes widely from very low power, even negative power in the case of vehicles, to relatively high power with a high rate of change. Thus, a generating system based only in a fuel cell would operate unfavourably most of the time in these applications.

Fuel Cell Hybrid Systems (FCHS) are composed of a primary power source, the fuel cell itself, and an energy storage system, a battery or supercapacitor bank, that contributes to supply the load power demand. Hence, the load power $P_{load}(t)$ is partly supplied from the fuel cell system, $P_{fcs}(t)$, and partly from the energy storage system, $P_{ess}(t)$, according to an established strategy, in such a way that:

$$P_{load}(t) = P_{fcs}(t) + P_{ess}(t) \quad \text{for all } t .$$

FCHS are particularly attractive due to the following advantages of hybridization [2, 3]: *i*) improvement of the hydrogen economy and the transient response using an efficient energy management strategy to coordinate the power split between the *Fuel Cell System (FCS)* and the *Energy Storage System (ESS)*, *ii*) size reduction of the *FCS*, *iii*) reduction of the cost and weight of the global system, *iv*) reduction of the warm-up time of the *FCS* to reach full power, and *v*) in the case of automotive applications, the possibility of improving the hydrogen consumption through the process of regenerative braking.

One important aspect of hybridization is the determination of the appropriate electrical topology. In [4, 5, 6, 7], studies based on different topologies and their appropriate control are made showing the advantages and disadvantages of each case. In Figure 1, it is shown the electrical topology that has been adopted in this work, where $P_{aux}(t)$ is the power consumed by the auxiliary system. The *FCS* is connected to the *DC* bus through a step-up power converter (Boost converter), whereas the *ESS* is connected to the *DC* bus through a bi-directional power converter (Buck-Boost converter). The load is fed through a *DC-AC* inverter.

In this work, we perform an analysis and a comparative study between different proposed *Energy Management Strategies (EMS)* oriented to *Fuel Cell-Hybrid Vehicles (FCHVs)*. The system in study is a *FCHV* powered by a *FCS* and an *ESS* consisting of a supercapacitor bank that can be charged both from the *FCS* and from the load through regenerative braking. The proposed strategies were tested using a *FCHV* model elaborated employing ADVISOR toolbox in Matlab (see [8, 9]).

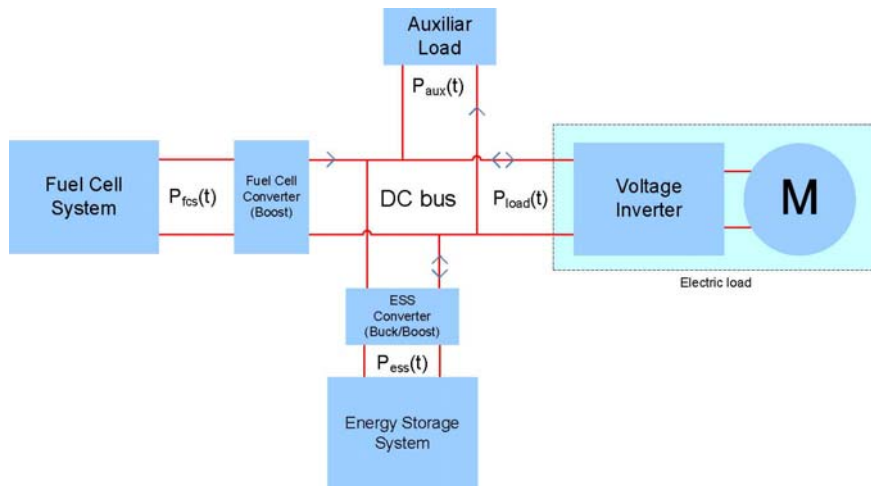


Figure 1 Electrical topology in the *FCHS* in study.

The structure of this paper is as follows: in Section 2, the *Fuel Cell Hybrid Vehicles* issue is addressed showing the advantages of hybridization, the case of study, the model, and the scheme of power flow between the subsystems. In section 3, the *Energy Management Strategies* are approached including a brief state of the art, the objectives, the cost function, the constraints, and the description of the proposed strategies. In Section 4, the simulation results are presented showing the methodology of analysis, the temporal response of the strategies and the comparative of its performances. In Section 5, the conclusions of the work are presented.

2. FUEL CELL HYBRID VEHICLES

Fuel Cell Hybrid Vehicles (FCHVs) is a promising technology able to reduce the total fuel consumption and greenhouse gas emissions, and achieve strictly zero exhaust pipe emissions. For the same performance, hydrogen fuel cell vehicles are likely to be simpler in design, lighter, more energy efficient, and less expensive than methanol or gasoline fuel cell vehicles. Moreover, the tailpipe emissions will be strictly zero under all operating conditions [10].

The advantages of *FCHVs* with respect to the pure fuel cell vehicles (i.e., when the fuel cell is the only power source), and complementary to the advantages of *FCHS* already explained, are:

- Reduction of the fuel cell stack thanks to the *ESS* power assistance which is translated in a reduction of the production costs.
- Improvement in the hydrogen economy through regenerative braking.
- Increase of the vehicle autonomy due to the hydrogen economy improvement.
- Increase of the efficiency of the fuel cell operation through an adequate energy management strategy.

The system in study is a *FCHV* powered by a *FCS* and an *ESS* consisting of a supercapacitor bank. The *FCS* is connected to the *DC* bus through a power converter and the *ESS* through a bidirectional power converter. The *ESS* can be charged both from the *FCS* and from the load through regenerative braking. In Figure 2 is showed an energy-flow scheme of the *FCHV* where are represented the regenerated energy from load to the *ESS*, the charging energy from the *FCS* to the *ESS*, the boosting energy from the *ESS* to the load, and the fuel cell energy that directly supplies the load.

2.1. *FCHV* Model

In order to formulate and evaluate appropriate energy-management-strategies in *Fuel Cell Hybrid Vehicles (FCHV)*, it is necessary to develop an adequate model able to represent the behaviour of the system. The model must be accurate enough to capture the system compartment but, at the same time, must be simple enough so that it is possible to use it for the analysis and validation of the energy management strategy in study. The *FCHV* system model is detached in three main sub-models: *i*) the *Fuel Cell*

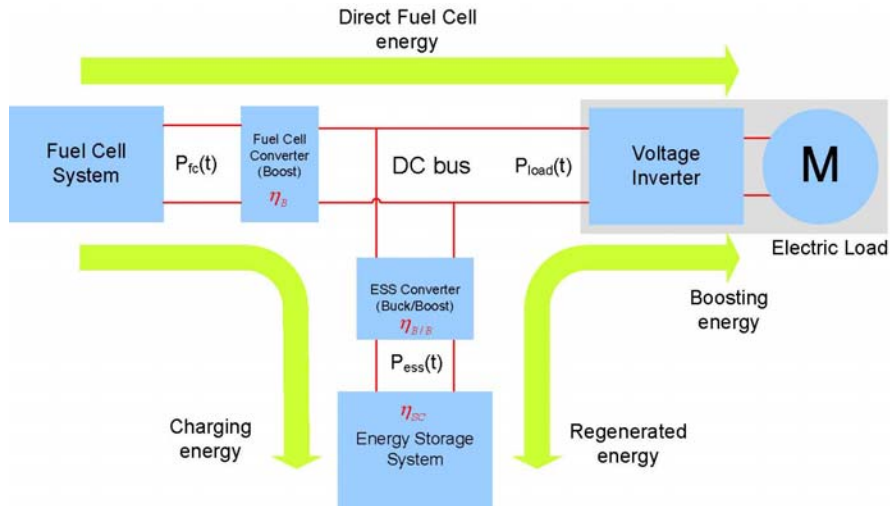


Figure 2 Energy-flow scheme in the *FCHV*

System model, *ii*) the *Energy Storage System* model and *iii*) the corresponding *Vehicle* model.

In this work, the *ADvanced VehIcle SimulatOR (ADVISOR)* is utilized to model the hybrid vehicle. *ADVISOR* is a toolbox created in the *MATLAB/Simulink* environment and developed by the National Renewable Energy Laboratory of the USA with the aim of analyzing the performance and fuel economy of conventional, electric, and hybrid vehicles. It provides a flexible and robust set of models, data, and script text files which are primarily used to quantify the fuel economy, energy losses, performance, and emissions of vehicles that use alternative technologies including fuel cell, batteries, supercapacitors, electric motors, and internal combustion engines in hybrid configurations [8, 9]. The vehicle in study in this work is a small car the principal parameters of which are listed in Table 1.

Table 1 Specifications in the vehicle model.

Specification	Value
Vehicle mass [§]	882 kg
Vehicle total mass	1093 kg
Frontal area	2 m ²
Drag coefficient	0.335
Coefficient of rolling friction	0.009
Air density	1.2 kg m ⁻³

[§]Vehicle mass without the FCS, the ESS, and converters.

Figure 3 shows the energy flow in a *FCHV* illustrating the energy interchange between the components that constitute the *FCHV* and the corresponding losses running with optimal generation in the *New European Driving Cycle (NEDC)*[†].

3. ENERGY MANAGEMENT STRATEGIES

The Energy Management Strategies are algorithms which determine at each sampling time the power generation split between the *Fuel Cell System (FCS)* and the *Energy Storage System (ESS)* in order to fulfil the power balance between the load power and the power sources. Depending on how the power split is done a minimization of the hydrogen consumption can be obtained. To find a global optimal solution, control techniques where a minimization problem is resolved have been studied [11]. In general, these techniques do not offer a causal solution, and in consequence are not feasible, because they assume that the future driving cycle is entirely known a priori. Nevertheless, their results can be used to compare with the performance of new strategies in study. On the other hand, strategies which deal with local optimization are convenient for real implementation. Another approach, particularly convenient to work in real time operation, is the type of strategies where the detailed knowledge of the

[†] *NEDC* is one of the standard driving cycles that are useful to evaluate vehicles performances. This cycle will be described in detail in Section 4.

system operation is exploited. These strategies can achieve a comparable performance to those strategies where some optimization technique is utilized.

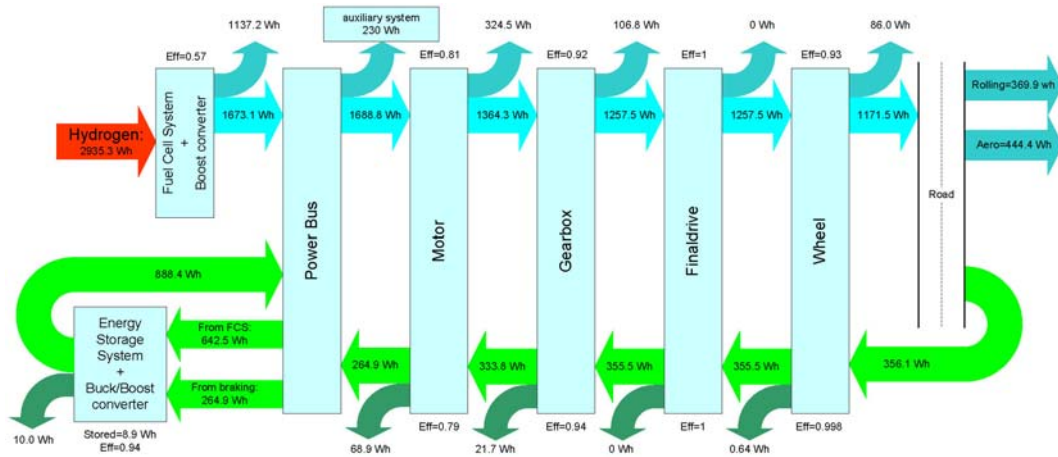


Figure 3 Energy flow in the FCHV running on NEDC.

Different approaches for *EMS* are found in literature. In [12], the proposed strategy is based on the regulation of the DC link voltage by controlling two power converters, and, thus, the fuel cell operates in almost steady state conditions. In [13], it is proposed a control strategy with two objectives: obtaining high efficiency in the hybrid system and maintaining the state of charge in the batteries above a minimum value. If both objectives cannot be fulfilled simultaneously, the priority is given to the battery state of charge. In [14], three heuristic strategies are compared using a *Fuel Cell Hybrid Vehicle* model. In contrast, other publications propose strategies based on optimization techniques. One of the most relevant is the method presented in [15], based on a control strategy called *Equivalent Consumption Minimization Strategy (ECMS)*. The base of this strategy consists in converting all the power flows in equivalent hydrogen consumptions. Using the same concept, in [16], a real time control is implemented on a

real fuel cell-supercapacitor-powered vehicle with good results. Other strategies based on optimization techniques are presented in [3, 17, 18, 19].

In this work, three strategies are presented: two strategies based on the knowledge of the fuel-cell efficiency map and one strategy based on constrained nonlinear programming. First of all, a cost function that quantifies the amount of hydrogen consumed in the fuel cell is enunciated.

One of the main advantages of *FCES* is the possibility to reduce the hydrogen consumption operating the *FCS* efficiently and taking advantage of the energy obtained from regenerative braking. Thus, one of the principal objectives of the management strategy is to minimize a cost function J , which represents the cumulative hydrogen consumption during driving cycle:

$$\min_X J(X) \quad \text{subject to} \quad H(X) = 0 \quad \text{and} \quad G(X) \leq 0,$$

where the vector X is:

$$X = \begin{bmatrix} P_{fcs}(t) \\ P_{ess}(t) \end{bmatrix}.$$

This means that the control strategy has to determine the optimal value of $P_{fcs}(t)$ and $P_{ess}(t)$ in order to minimize the cost function $J(X)$:

$$J(X) = \int_0^{t_c} F(X) dt,$$

where t_c is the duration of the driving cycle and $F(X)$ is the hydrogen consumption according to the hydrogen consumption map of the *FCS*:

$$F(X) = \text{Cons}_{H_2}(P_{fcs}(t)).$$

A graphic showing the hydrogen consumption is presented in Figure 4.

The constraint $H(X) = 0$ states the condition that at every time the power balance in the *DC* bus must be satisfied:

$$P_{fcs}(t) \cdot \eta_B + P_{ess}(t) \cdot \eta_{B/B} = P_{load}(t) \quad \forall t \in [0, t_c].$$

On the other hand, the constraint $G(X) \leq 0$ states the constraints in the *FCS* and the *ESS*:

$$\begin{aligned} P_{fcs, \min} &\leq P_{fcs}(t) \leq P_{fcs, \max} \\ \Delta P_{fcs, \min} = \Delta P_{fcs, \text{fall rate}} &\leq \frac{dP_{fcs}(t)}{dt} \leq \Delta P_{fcs, \max} = \Delta P_{fcs, \text{rise rate}} \\ P_{ess, \min}(SoE(t)) &\leq P_{ess}(t) \leq P_{ess, \max}(SoE(t)) \\ SoE_{\min} &\leq SoE(t) \leq SoE_{\max} \end{aligned}$$

for all $t \in [0, t_c]$, where the *State of Energy* $SoE(t)$ in the *ESS* is defined as:

$$SoE(t) := \frac{E_{ess}(t)}{E_{cap}} \times 100 \quad [\%]$$

and E_{cap} is the maximum energy that the storage system is capable to store. The maximum *ESS* power that is possible to supply or store depends on the actual voltage in the *ESS*, $V_{ess}(t)$, the maximum voltage $V_{ess, \max}$, and the minimum voltage $V_{ess, \min}$:

$$\begin{aligned} P_{ess, \text{chrg max}}(t) &= \frac{(V_{ess}(t) - V_{ess, \max})}{R_d} \cdot V_{ess}(t) \quad \text{during charging} \\ P_{ess, \text{disch max}}(t) &= \frac{(V_{ess}(t) - V_{ess, \min})}{R_d} \cdot V_{ess}(t) \quad \text{during discharging,} \end{aligned}$$

where R_d is the *ESS* internal resistance. The charge voltage is related with the *ESS* energy, so that it is possible to express $P_{ess}(t)$ as a function of $SoE(t)$:

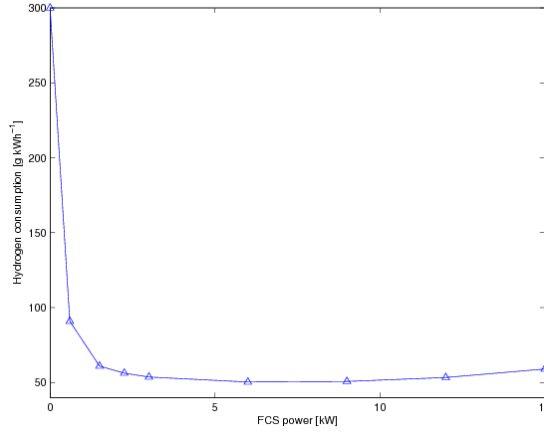


Figure 4 Hydrogen consumption map as a function of the FCS power for a 15 kW stack FCS

$$P_{ess, chrg\ max}(t) = k_{ess} \cdot (SoE(t) - SoE_{\max})$$

$$P_{ess, dischr\ max}(t) = k_{ess} \cdot (SoE(t) - SoE_{\min}),$$

where:

$$k_{ess} = \frac{k \cdot E_{cap}}{R_d \cdot C_R} \quad (1)$$

is the constant that relates the actual *SoE* and the power that the device can supply or store. Thus, $P_{ess, chrg\ max}(t)$ is the maximum power that the *ESS* is capable to store at the instant t (charging mode) and the $P_{ess, dischr\ max}(t)$ is the maximum power that the *ESS* is capable to supply at instant t (discharging mode). According to the sign convention employed in this work, the power is negative when the *ESS* is in charging mode, meanwhile it is positive when the *ESS* is discharging mode. The k_{ess} constant depends on the *DC* internal resistance R_d , the supercapacitor capacitance C_R , and the constant k depending on the particular supercapacitor technology. The internal resistance of supercapacitors is extremely low and the capacitance is exceptionally high, allowing a

very fast operation both during charging and discharging. In the employed supercapacitors they are: $R_d = 0.019\Omega$ and $C_R = 58 F$, thus, $k_{ess} = 479 kW$.

3.1. Strategy based on efficiency map

One of the most relevant characteristic of a *FCS* is the efficiency map (see Figure 5) which shows how the efficiency changes with the load power. It is supposed that the *FCS* is controlled and, thus, external parameters such the ambient temperature have no influence in the efficiency map.

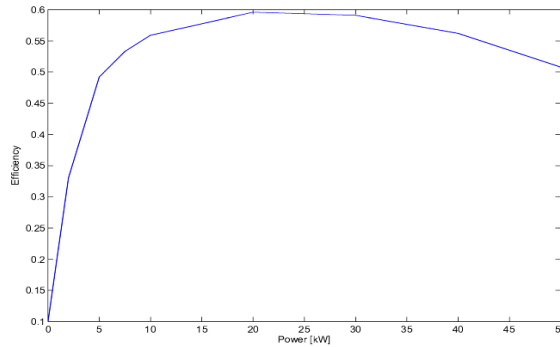


Figure 5 50 kW Fuel Cell efficiency curve from ADVISOR.

The first strategy proposed in this work is a *quasi-load-following*[‡] strategy where the fuel cell is operated in an advantageous zone where the efficiency is high. In this case, the operating zone is constrained between an inferior limit ($P_{fcs, lo}$) and a superior limit ($P_{fcs, hi}$). The superior limit is imposed by the maximum power that the fuel cell can deliver (i.e., $P_{fcs, hi} = P_{fcs, max}$), whereas the inferior limit is determined according to the efficiency curve. As we mentioned before, the efficiency of a *FCS* at low power is very poor due to the parasitic power. Thanks to the inferior limit, the energy management strategy avoids this unfavourable zone.

[‡] A *load-following* strategy is a strategy that adjusts the power output of the fuel cell according to the load requirement.

Considering the losses in the power converters (η_B and $\eta_{B/B}$), and assuming that the *ESS* efficiency is a constant, η_{ess} , the power balance in the *DC* bus, can be rewritten as:

$$P_{fcs}(k) \cdot \eta_B + P_{ess}(k) \cdot \eta_{B/B} \cdot \eta_{ess} = P_{load}(k) \quad k = 1, 2, \dots, N_c,$$

where $N_c = t_c / \Delta T$ is the cycle duration, assuming a constant sampling period $\Delta T = 1$ s.

Consequently, given the present $P_{load}(k)$, if:

$$P_{fcs, lo} \cdot \eta_B \leq P_{load}(k) \leq P_{fcs, max} \cdot \eta_B$$

and

$$\Delta P_{fcs, fall rate} \leq \Delta P_{load}(k) \leq \Delta P_{fcs, rise rate},$$

where

$$\Delta P_{load}(k) = P_{load}(k) - P_{load}(k-1),$$

then, the *FCS* operates in load-following mode:

$$P_{fcs}(k) = P_{load}(k) / \eta_B \quad (2a)$$

and

$$P_{ess}(k) = 0.$$

If, on the contrary:

$$P_{load}(k) \leq P_{fcs, lo}(k) \cdot \eta_B,$$

then:

$$P_{fcs}(k) = P_{fcs, lo}(k) \quad (2b)$$

and, the *ESS* stores the rest of generated power, if the *ESS* is not too charged:

$$P_{ess}(k) = -\min \left\{ \left| P_{load}(k) - P_{fcs}(k) \cdot \eta_B \right| \cdot \eta_{B/B} \cdot \eta_{ess}, \left| SoE(k) - SoE_{max} \right| \cdot k_{ess} \right\}, \quad (3)$$

Conversely, if:

$$P_{load}(k) \geq P_{fcs, hi}(k) \cdot \eta_B,$$

then:

$$P_{fcs}(k) = P_{fcs, \max},$$

and, the *ESS* supplies the rest of load power, if there is enough energy in *ESS*:

$$P_{ess}(k) = \min \left\{ \frac{(P_{load}(k) - P_{fcs}(k) \cdot \eta_B)}{\eta_{B/B} \cdot \eta_{ess}}, (SoE(k) - SoE_{\min}) \cdot k_{ess} \right\}. \quad (4)$$

In Figure 6, it is represented how is determined the *FCS* operating point. However, the transition between operating points is limited by the maximum rates, thus:

$$P_{fcs}(k) = \begin{cases} P_{fcs}(k-1) + \Delta P_{fcs, \text{rise rate}} \cdot \Delta T, & \text{if } \Delta P_{fcs}(k) \geq \Delta P_{fcs, \text{rise rate}} \\ P_{fcs}(k-1) + \Delta P_{fcs, \text{fall rate}} \cdot \Delta T, & \text{if } \Delta P_{fcs}(k) \geq |\Delta P_{fcs, \text{fall rate}}| \end{cases}, \quad (5)$$

where $\Delta P_{fcs} = P_{fcs}(k) - P_{fcs}(k-1)$, with $P_{fcs}(k)$ as it was previously calculated in (2a) or (2b).

The power $P_{ess}(k)$ is calculated as is indicated in (3) and (4).

3.2. Improved strategy based on the efficiency map

The second strategy based on the *FCS* efficiency map is a strategy which operates the *FCS* preferably in its point of maximum efficiency in order to improve the hydrogen economy. The operating point of the *FCS* is determined based on the actual power demand and state of energy of the *ESS*. The *FCS* power command is determined according to the following rules. If the load power is:

$$P_{fcs, lo} \cdot \eta_B \leq P_{load}(k) \leq P_{fcs, hi} \cdot \eta_B$$

and, the *SoE* is:

$$SoE_{lo} \leq SoE(k) \leq SoE_{hi},$$

where $P_{fcs, hi}$ is:

$$P_{fcs, hi} = P_{fcs, max} \cdot \eta_B \cdot X_{fcs, hi} ,$$

and $X_{fcs, hi}$ is a fraction of the maximum FCS power, then, the FCS is operated in its point of maximum efficiency:

$$P_{fcs}(k) = P_{fcs, max\ eff} \cdot$$

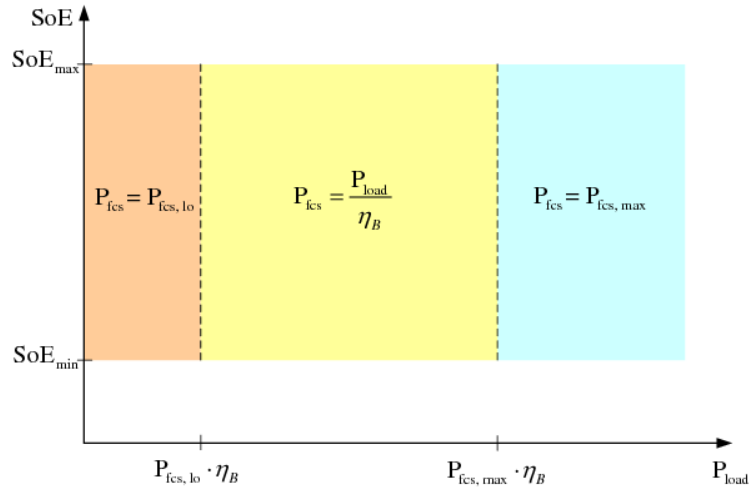


Figure 6 FCS operating point as a function of the SoE in the ESS and the load power.

The remaining power to achieve the load demand flows from or to the ESS according to (3) if $P_{load}(k) > P_{fcs, max\ eff}$ (discharging mode), or (4) if $P_{load}(k) < P_{fcs, max\ eff}$ (charging mode).

If the load power is:

$$P_{fcs, hi} \cdot \eta_B \leq P_{load}(k) \leq P_{fcs, max} \cdot \eta_B$$

and, the SoE is:

$$SoE_{lo} \leq SoE(k) \leq SoE_{hi} ,$$

then, the FCS is operated in load following mode:

$$P_{fcs}(k) = P_{load}(k) / \eta_B,$$

and $P_{ess}(k)$ is as indicated in (3) or (4).

On the other hand, if:

$$P_{load}(k) \geq P_{fcs, \max} \cdot \eta_B \quad \text{and} \quad SoE(k) \leq SoE_{hi},$$

or:

$$SoE(k) \leq SoE_{lo},$$

then, the *FCS* is operated at its maximum power:

$$P_{fcs}(k) = P_{fcs, \max},$$

and $P_{ess}(k)$ is as indicated in (3). If, on the contrary:

$$P_{load}(k) \leq P_{fcs, lo} \cdot \eta_B \quad \text{and} \quad SoE(k) \geq SoE_{lo},$$

or:

$$SoE(k) \geq SoE_{hi},$$

then, the *FCS* is operated at its lower operating point:

$$P_{fcs}(k) = P_{fcs, lo},$$

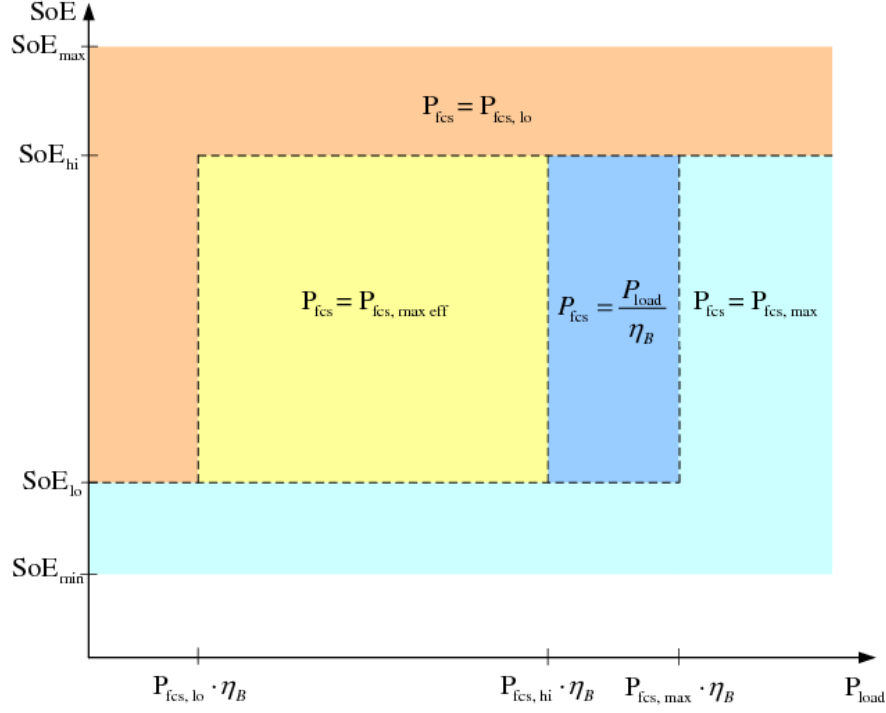


Figure 7 FCS operating point as a function of the *SoE* in the *ESS* and the load power.

and $P_{ess}(k)$ is as in (4). Additionally, if $P_{load}(k)=0 \forall t \in [k_1, k_2]$ with $k_2-k_1 > T_{off}$, and, $SoE(k) > SoE_{hi} \quad k > k_2$, then, the *FCS* is turned off to avoid unnecessary hydrogen consumption because the parasitic losses in the *FCS*. Figure 7 indicates the *FCS* operating point as a function of the $SoE(k)$ in the *ESS* and the load power $P_{load}(k)$. In the same way that in the previous strategy, the transition between operating points is realized according to the constraints concerning the maximum fall power rate and the maximum rise power rate as indicated in (5).

3.3. Strategy based on constrained nonlinear programming

In this strategy, an optimization problem with linear constraints is resolved at each sampling period ΔT where a nonlinear cost function, which represents the hydrogen consumption, is minimized. The problem can be put into the form [20]:

$$\min_X J(X) \quad \text{subject to} \quad H(X) = 0 \quad \text{and} \quad G(X) \leq 0,$$

where the vector X is:

$$X = \begin{bmatrix} P_{fcs} \\ P_{ess} \end{bmatrix}.$$

The cost function $J(X)$ represents the hydrogen consumption in the FCS :

$$J(X) = F(P_{fcs}(k)),$$

where:

$$F(P_{fcs}(k)) = ConsH_2(P_{fcs}(k)) \cdot P_{fcs}(k) \cdot \Delta T,$$

and $ConsH_2(P_{fcs}(k))$ is the hydrogen consumption ($g Wh^{-1}$) as a function of $P_{fcs}(k)$. This relationship is shown in the form of a consumption map in Figure 4.

The set of constraints $H(X) = 0$ represents the power balance in the DC bus:

$$P_{fcs}(k) \cdot \eta_B + P_{ess}(k) \cdot \eta_{B/B} \cdot \eta_{ess} = P_{load}(k) \quad k = 1, 2, \dots, N_c$$

and the set of constraints $G(X) \leq 0$ represents the limitations in $P_{fcs}(k)$ and $P_{ess}(k)$. The $P_{fcs}(k)$ is limited in its maximum and minimum value, and in the maximum rise rate and fall rate,

$$P_{fcs, lo} \leq P_{fcs}(k) \leq P_{fcs, hi},$$

and:

$$P_{fcs}(k-1) + \Delta P_{fcs, fall\ rate} \cdot \Delta T \leq P_{fcs}(k) \leq P_{fcs}(k-1) + \Delta P_{fcs, rise\ rate} \cdot \Delta T.$$

This can be rewritten as:

$$P_{fcs, min}(k) \leq P_{fcs}(k) \leq P_{fcs, max}(k),$$

where:

$$P_{fcs, \max}(k) = \min \left\{ P_{fcs, hi}; P_{fcs}(k-1) + \Delta P_{fcs, fall\ rate} \cdot \Delta T \right\}$$

$$P_{fcs, \min}(k) = \max \left\{ P_{fcs, lo}; P_{fcs}(k-1) + \Delta P_{fcs, rise\ rate} \cdot \Delta T \right\}.$$

On the other hand, $P_{ess}(k)$ is limited to its maximum or minimum value depending on the actual $SoE(k)$. The $SoE(k)$ is limited:

$$SoE_{\min} \leq SoE(k) \leq SoE_{\max},$$

thus:

$$k_{ess} \cdot (SoE(k) - SoE_{\max}(k)) \leq P_{ess}(k) \leq k_{ess} \cdot (SoE(k) - SoE_{\min}(k)),$$

where k_{ess} is the constant defined in (1).

4. RESULTS

The enunciated strategies were tested in a hybrid system consisting in the vehicle previously described in Table 1, provided with a FCS and a supercapacitors-based ESS with the principal parameters listed in Table 2.

Table 2 Simulation parameters used to test the energy management strategies.

Parameter	Symbol	Value
Number of supercapacitors	N_{cap}	250
Maximum ESS energy	$E_{ess, \max}$	612 Wh
Maximum SoE	SoE_{\max}	1
Minimum SoE	SoE_{\min}	0.2
High limit of SoE	SoE_{hi}	0.9
Low limit of SoE	SoE_{lo}	0.3
Maximum ESS power	$P_{ess, \max}$	255 kW
Maximum FCS power	$P_{fcs, \max}$	15 kW
Maximum FCS rise rate power	$\Delta P_{fcs, rise\ rate}$	600 W s ⁻¹
Maximum FCS fall rate power	$\Delta P_{fcs, fall\ rate}$	-900 W s ⁻¹
Maximum FCS efficiency	$\eta_{fcs, \max}$	0.6
FCS power of maximum efficiency	$P_{fcs, \max\ eff}$	6 kW
Energy storage efficiency	η_{ess}	0.99
Boost converter efficiency	η_B	0.95
Buck/Boost converter efficiency	$\eta_{B/B}$	0.95

The parameters $P_{fcs, lo}$ and $P_{fcs, hi}$ act as adjustment parameters, allowing to improve the fuel economy and performance according to the particular strategy and cycle. These parameters are shown in Table 3.

Table 3 Values of the parameters $P_{fcs, lo}$ and $P_{fcs, hi}$.

	$P_{fcs, lo}$ [kW]	$P_{fcs, hi}$ [kW]
Strategy based on efficiency map	1	15
Improved strategy based on efficiency map	1	12
Strategy based on nonlinear programming	2	15

The strategies are tested on four different driving cycles: the *New European Driving Cycle (NEDC)*, the *Urban Dynamometer Driving Schedule (UDDS)*, the *Federal Test Procedure (FTP)*, and the *Highway Fuel Economy Test (HWFET)*. These standard driving cycles were originally stated for measuring pollutant emissions and gasoline economy of engines and represent typical driving scenarios concerning speed and acceleration.

4.1. Simulation results

Firstly, the simulation results corresponding to the three strategies are shown: the power split between the fuel cell system and the energy storage system, and the evolution of the $SoE(t)$ in the *ESS* are shown in Figure 8 to Figure 10 for the *NEDC* cycle. Secondly, a comparative between the corresponding performances for the four cycles is done.

4.2. Comparative

The comparative between the performances of the strategies, in terms of hydrogen consumption per kilometre, is done in Figure 11. The comparative is done between the performance of the three strategies with respect to the corresponding to the optimal case

where the consumption is minimum; the values in percentages indicate the increment in consumption with respect to the optimal case. The performance of the optimal case is estimated assuming that the entire cycle is known a priori.

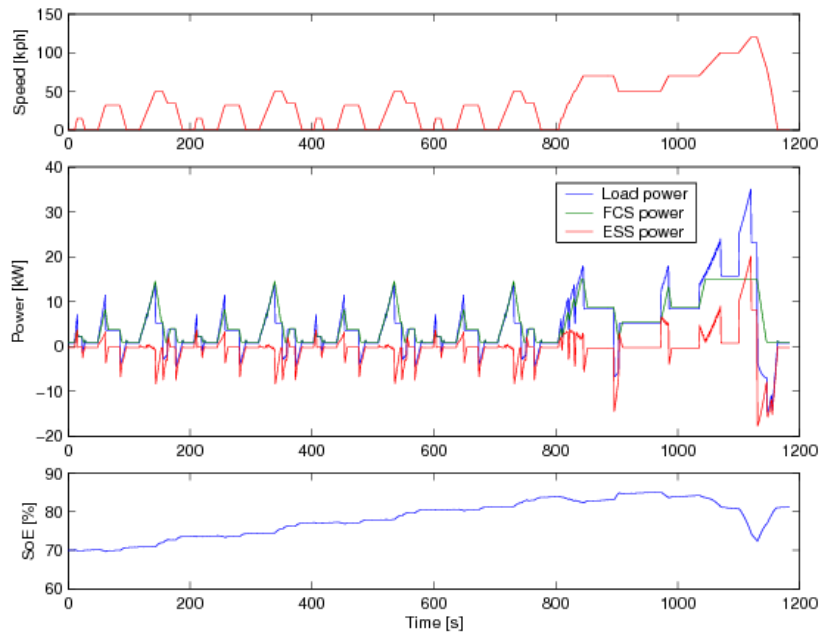


Figure 8 Power split between the FCS and the ESS to meet the load power to fulfil the NEDC, and the evolution of *SoE* in the *ESS* testing the strategy based on efficiency map.

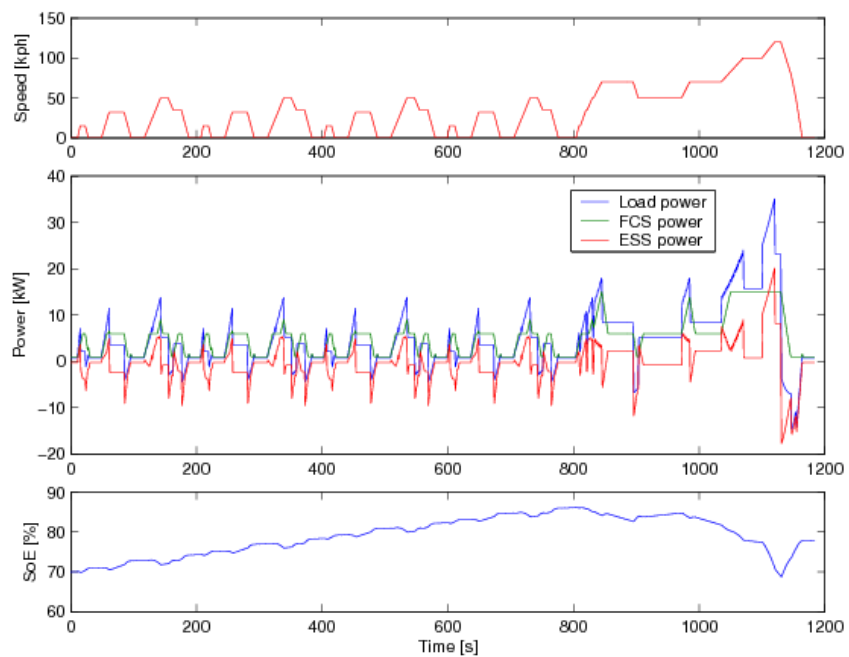


Figure 9 Power split between the FCS and the ESS to meet the load power to fulfil the NEDC, and the evolution of *SoE* in the *ESS* testing the improved strategy based on efficiency map.

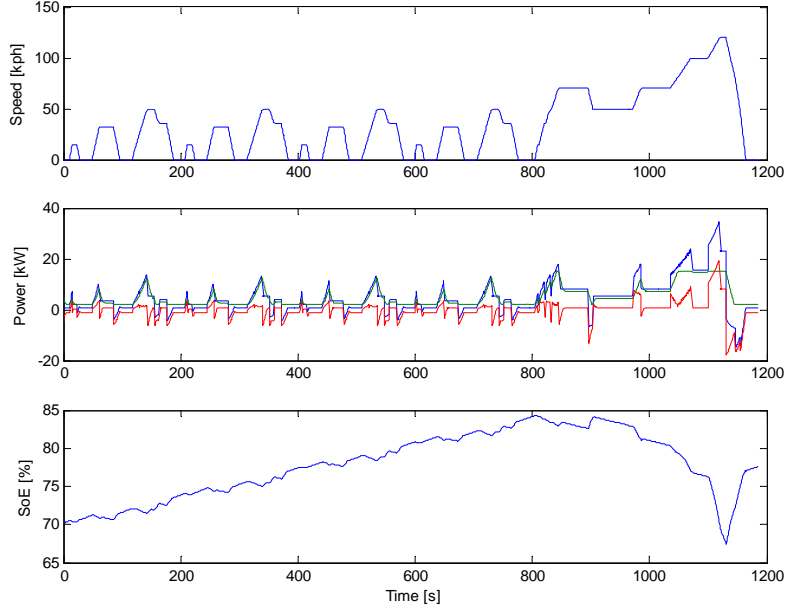


Figure 10 Power split between the FCS and the ESS to meet the load power to fulfil the NEDC, and the evolution of SoE in the ESS testing the strategy based on constrained nonlinear programming.

Thus, it is possible to operate the fuel cell during the entirely cycle at its point of maximum efficiency. In addition, in Figure 11 is included the performance corresponding to the FCS pure case where there is no hybridization. The analysis of the FCS pure case is performed with a 37.5 kW-FCS, which is sufficient to fulfil the four cycles in study.

In general, the final state of charge $SoE(N_c)$ is different to the initial $SoE(0)$, resulting in a gain or a loss of energy in the ESS over the driving cycle. Because of that, the results are corrected in order to compare the results correctly. The corrected consumption of hydrogen is based on the assumption that after the cycle, the FCS is continuing running in its point of maximum efficiency until the SoE reaches again the initial value. Thus, the corrected consumption results:

$$Cons_{H_2, corrected} = Cons_{H_2} + \frac{\Delta E_{ess, stored}}{LHV_{H_2} \cdot \eta_{fcs, max} \cdot \eta_{ess} \cdot \eta_B \cdot \eta_{B/B}}$$

where, $Cons_{H_2}$ is the cumulative consumption of hydrogen over the cycle previous to the correction, $\Delta E_{ess, stored}$ is the difference of the energy stored in the ESS at the end of the cycle with the energy at the beginning of the cycle (positive if the $SoE(N_c)$ is larger than the $SoE(0)$ and negative in the opposite situation), LHV_{H_2} is the low heating value of hydrogen, and $\eta_{fcs, max}$ is the maximum efficiency of the FCS .

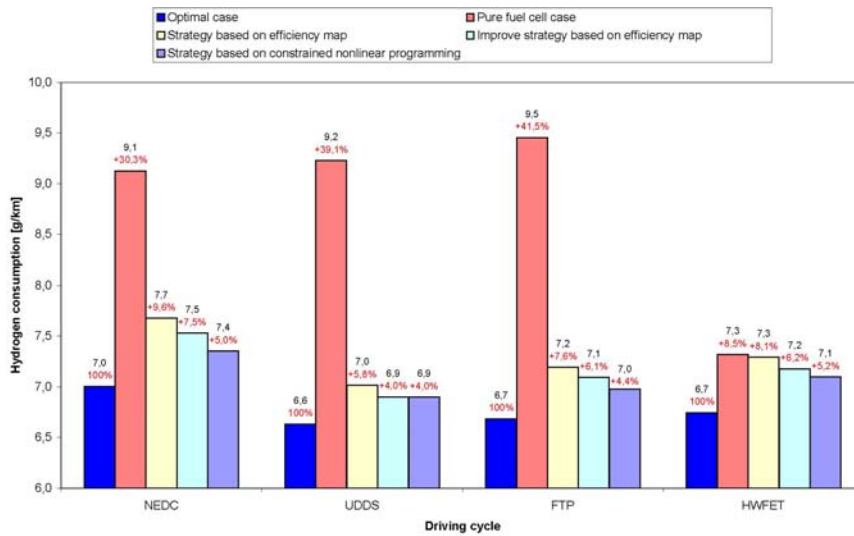


Figure 11 Comparative between the hydrogen consumption of the proposed strategies and the FCS pure case with respect to the optimum case.

5. DISCUSSION

The analysis of the hydrogen economy in Figure 11 shows that the three strategies have a good performance compared to the optimal case where the entire driving cycle is known a priori, which is not feasible in practice. In fact, the maximum deviation from the optimal case is 9.6% in the strategy based on efficiency map running on $NEDC$. The strategy based on constrained nonlinear programming gives the best performance in all the cases; however, the performance is similar to the two strategies based on efficiency map. On the other hand, compared to the pure fuel cell case in Figure 12, the results

show considerable hydrogen savings running on cycles *NEDC*, *UDDS*, and *FTP*. On the contrary, running on *HWFET* the savings is exiguous. This cycle is a highway driving cycle and one of its characteristic is that the average deceleration is significantly lower (-0.22 m s^{-2}) than the corresponding to the other cycles (*NEDC*: -0.79 m s^{-2} ; *UDDS*: -0.58 m s^{-2} ; *FTP*: -0.58 m s^{-2}). These results suggest that the strategies achieve the objectives satisfactorily when a significant energy is recovered from braking.

It is remarkable that it is possible to meet the load power in the four driving cycles with a *FCS* of 15 kW that is significantly lower to the corresponding in the pure fuel cell case with no hybridization (37.5 kW) which is translated in a cost-producing reduction. This is possible thanks to the *ESS* power assistance in the proposed strategies.

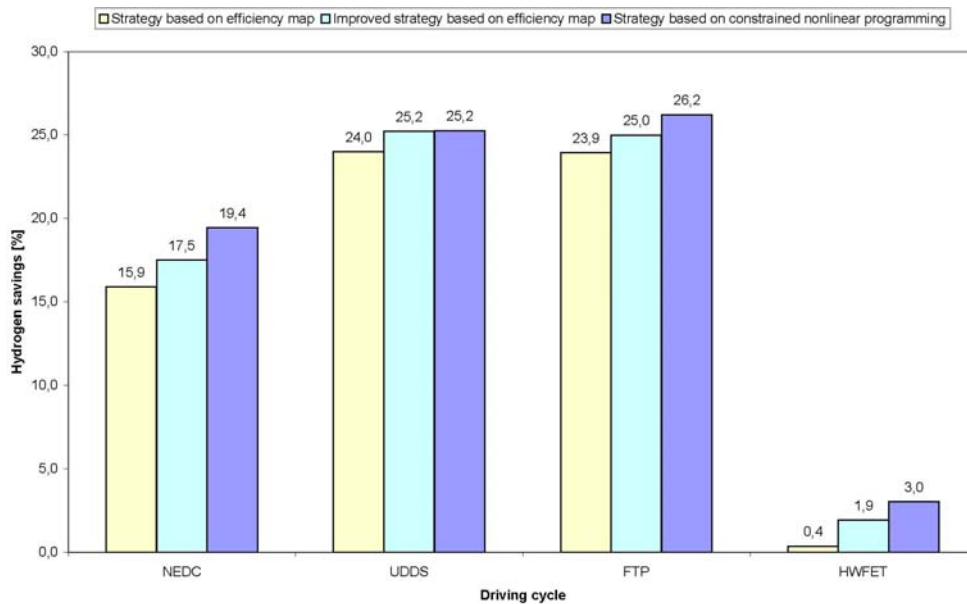


Figure 12 Hydrogen savings with respect to the pure fuel cell case.

6. CONCLUSIONS

In this work, three energy management strategies for *Fuel Cell Hybrid Systems* are presented. Two of them are based on the knowledge of the fuel cell efficiency map. The

third strategy is based on constrained nonlinear programming. The system in study is a *Fuel Cell Hybrid Vehicle* powered by a fuel cell and a supercapacitor bank with the possibility of regenerating energy from braking. The performances of the strategies are analyzed using the ADVISOR toolbox which allows to model in detail the system in study. The simulation results include the analysis of the performance of the strategies running on four different driving cycles. The comparative of the performance is done with respect to the optimal case where the hydrogen consumption is minimal. Besides, the pure fuel cell case is included to analyze the improvement in the hydrogen economy due to hybridization. The results indicate a good performance on the three strategies, near to the optimal case, improving the hydrogen economy and allowing the reduction of the fuel cell stack size.

Acknowledgments

This work has been funded partially by the project CICYT DPI2007-62966 of the Spanish Government, and the support of a PhD doctoral grant of the Department of Universities, Investigation and Society of Information of the Generalitat de Catalunya.

Glossary

$Cons_{H_2}$	Hydrogen consumption
C_R	Capacity of the supercapacitors
E_{cap}	Capacity of energy storage in the <i>ESS</i>
<i>ESS</i>	Energy Storage System
<i>FCHS</i>	Fuel Cell Hybrid System
<i>FCHV</i>	Fuel Cell Hybrid Vehicle
<i>FTP</i>	Federal Test Procedure
<i>HWFET</i>	Highway Fuel Economy Test
k_{ess}	Constant between power and <i>SoE</i> in the <i>ESS</i>

LHV_{H2}	Low Heating Value of hydrogen
$NEDC$	New European Driving Cycle
$PEMFC$	Proton Exchange Fuel Cell
P_{aux}	Power consumed by the auxiliary system
P_{ess}	Power supplied by the <i>ESS</i>
P_{fcs}	Power supplied by the <i>FCS</i>
P_{load}	Power required by the load
R_d	Internal resistance of the supercapacitors
SoE	State of Energy in the <i>ESS</i>
$UDDS$	Urban Dynamometer Driving cycle
$\Delta P_{fcs, fall\ rate}$	Maximum <i>FCS</i> fall rate power
$\Delta P_{fcs, rise\ rate}$	Maximum <i>FCS</i> rise rate power
ΔT	Sampling period
η_B	Boost converter efficiency
$\eta_{B/B}$	Buck/boost converter efficiency
η_{ess}	<i>ESS</i> efficiency

References

- [1] P. Zegers, *Journal of Power Sources*, 15 (2006) 497-502.
- [2] K. Jeong, B. Oh, *Journal of Power Sources*, 105 (2002) 58-65.
- [3] P. Rodatz, G. Paganelli, A. Sciarretta, L. Guzzella, *Control Engineering Practice*, 13 (2004) 41-53.
- [4] K. Rajashekara, *Fuel Cell Technology for Vehicles*, (2000) 179-187.
- [5] A. Drolia, P. Jose, N. Mohan, *Industrial Electronics Society*, 1 (2003) 897-901.
- [6] K. Rajashekara, *Industrial Electronics Society*, 3 (2003) 2865-2870.
- [7] E. Santi, D. Franzoni, A. Monti, D. Patterson, N. Barry, *Applied Power Electronic Conference and Exposition*, (2002) 605-613.
- [8] T. Markel, A. Brooker, T. Hendricks, V. Johnson, K. Kelly, B. Kramer, M. O'Keefe, S. Sprik, K. Wipke, *Journal of Power Sources*, 110 (2002) 255-266.
- [9] K. Wipke, M. Cuddy, S. Burch, *IEEE Transactions on Vehicular Technology*, 48 (1999) 1751-1761.
- [10] J.M. Ogden, M.M. Steinbugler, T.G. Kreutz, *Journal of Power Sources*, 79 (1999) 143-168, 1999
- [11] J. Kessels. *Energy Management for Automotive Power Nets*. PhD thesis, Technische Universiteit Eindhoven, 2007.
- [12] P. Thounthong, S. Raël, B. Davat, *Journal of Power Sources*, 158 (2006) 806-814.
- [13] J. Jung, Y. Lee, J. Loo, H. Kim, *Fuel Cell for Transportation*, (2003) 201-205.
- [14] J. Schiffer, O. Bohlen, RW de Doncker, DU Sauer, *Vehicle Power and Propulsion*, 2005 IEEE Conference, (2005) 716-723.
- [15] G. Paganelli, Y. Guezennec, G. Rizzoni, in *SAE International*, 2002, pp. 71-79.
- [16] P. Rodatz, O. Garcia, L. Guzzella, F. Büchi, M. Bärschi, T. Tsukada, P. Dietrich, R. Kotz, G. Schreder A. Woukan, *Fuel Cell Power for Transportation*, (2003) 77-84.
- [17] S. Caux, J. Lachaize, M. Fadel, P. Shott, L. Nicod, *Journal of Process Control*, 15 (2004) 481-491.
- [18] S. Caux, J. Lachaize, M. Fadel, P. Shott, L. Nicod, In *Proceedings of the 16th IFAC World Congress*, Prague, 2005
- [19] M. Kim, H. Peng, *Journal of Power Sources*, 165 (2007) 819-832.
- [20] P. Gill, W. Murray, M. Wright, *Practical optimization*, tenth ed., Academic Press, London, 1981.